Ricobendazole nanocrystals obtained by media milling and spray drying: Pharmacokinetic comparison with the micronized form of the drug

Alejandro J. Paredes[a,1], Nahuel M. Camacho[a], Laureano Schofs[b], Alicia Dib[c], María del Pilar Zarazaga[d], Nicolás Litterio[d], Daniel A. Allemandi[a], Sergio Sánchez Bruni[b], Carlos Lanusse[b], Santiago D. Palma[a,*]

[a] Unidad de Investigación y Desarrollo en Tecnología Farmacéutica (UNITEFA), CONICET and Departamento de Ciencias Farmacéuticas, Facultad de Ciencias Químicas, Universidad Nacional de Córdoba, Haya de la Torre y Medina Allende, X5000XHUA Córdoba, Argentina
[b] Centro de Investigación Veterinaria de Tandil (CIVETAN-CONICET-CICPBA), Fac. Cs. Veterinarias, UNCPBA, Laboratorio de Farmacología, Departamento de Fisiopatología, Campus Universitario, Los Ombúes y Reforma Universitaria, Tandil, Argentina
[c] Departamento de Clínicas y Hospital Veterinario, Facultad de Veterinaria, Universidad de la República, Alberto Lasplaces 1620, 11600 Montevideo, Uruguay
[d] IRNASUS CONICET-Universidad Católica de Córdoba, Facultad de Ciencias Agropecuarias, Av. Armada Argentina, 3554, CP X5016DHK Córdoba, Argentina

ARTICLE INFO

ABSTRACT

Helminthic infections are produced by different types of worms and affect millions of people worldwide. Benzimidazole compounds such as ricobendazole (RBZ) are widely used to treat helminthiasis. However, their low aqueous solubility leads to poor gastrointestinal dissolution, absorption and potential lack of efficacy. The formulation of nanocrystals (NCs) have become the strategy of preference for hydrophobic drugs. In this work, we prepared RBZ NCs (RBZ-NCs) by an optimized combination of bead milling and spray-drying. Following the physicochemical characterization, a comparative pharmacokinetic evaluation of RBZ-NCs was performed in dogs using as controls a micronized powdered form of RBZ (mRBZ) and a physical mixture of drug and stabilizer 1:1 (PM). The particle size of the redispersed RBZ-NCs was 181.30 ± 5.93 nm, whereas DSC, PXRD and FTIR analyses demonstrated that the active ingredient RBZ remained physicochemically unchanged after the manufacture process. RBZ-NCs exhibited improved in vitro biopharmaceutical behaviour when compared to mRBZ. Consequently, the pharmacokinetic trial demonstrated a significant increase in the drug oral absorption, with an $AUC_{0-\infty}$ 1.9-fold higher in comparison to that obtained in animals treated with mRBZ. This novel formulation holds substantial potential for the development of new/alternative treatments for helminth infections both in human and veterinary medicine.

1. Introduction

Small animals like dogs and cats have been human companions for more than 10,000 years, and in the modern urbanized world they are often considered as "family members", even sharing family housing (Esch and Petersen, 2013). Nevertheless, they can host a series pathogens such as viruses, bacteria, fungi and parasites that can endanger humans health, with special emphasis being placed on helminths since they are extremely well-adapted for reproduction/infection and are highly prevalent in small animals (Chomel, 2008). On the other hand, some of these worms can infect human hosts producing zoonoses like human toxocariasis (Toxocara spp) or hydatid cyst (Echinococcus spp), a worldwide distributed condition that can cause even death where left untreated (WHO/OIE, 2002). Moreover, soil-transmitted helminth parasites currently affect 1.5 billion people worldwide (WHO, 2020)

Benzimidazolic antihelmintics (BZs) are a group of broad spectrum drugs widely used for the treatment of a variety of parasitic diseases in humans and animals (Lacey, 1990). Despite that, the hydrophobic

nature of these compounds, leads to poor gastrointestinal absorption and potentially to therapeutic failure (Page, 2008). When administered orally, BZs are dissolved in the stomach due to their weak basicity, absorbed in the duodenum and distributed to the entire body, reaching parasites dwelling in different tissues (Lanusse and Prichard, 1993). Albendazole (ABZ), is a BZ drug with extremely low aqueous solubility and after oral administration, it is completely transformed by first-pass effect to an active metabolite, albendazole sulphoxide, also named ricobendaozole (RBZ). Even though the slightly higher water solubility of RBZ makes it a good candidate for the development of alternative antiparasitic treatments, it is still hydrophobic and some proof of concept experiments have been carried out aiming at improving its *in vitro* and *in vivo* performance. For instance, Permana et al. designed solid lipid nanoparticles for intradermal administration (Permana et al., 2019), whereas other authors aimed at oral treatments using lipidic and polymeric nanoparticles (Ahmadnia et al., 2013; Naseri et al., 2016).

Among the strategies used to overcome the obstacle of poor water solubility of active pharmaceutical ingredients, the formulation of nanocrystals (NCs) has become the strategy of preference (Mohammad et al., 2019). NCs have unique physicochemical properties such as increased saturation solubility, dissolution rate and mucoadhesion, thus leading to an improved bioavailability and therapeutic efficacy (Mauludin et al., 2009; Gao et al., 2012). Drug nanosuspensions (NSs) can be produced by both, the bottom-up and the top-down approaches, being the second group of techniques the most easily reproducible and scalable, whereas the first approach is often limited by the use of organic solvents, which will ultimately remain in the formulation (Möschwitzer, 2013). Among the top-down techniques, media milling has been largely used to elaborate NCs, allowing to obtain nanometric and narrowly distributed particle sizes (Romero et al., 2016). After the milling process, further water removal of NSs can be performed to produce solid redispersible NCs using spray drying or lyophilisation (Hou et al., 2017; Touzet et al., 2018).

Our research group has been working on the development of formulations such as solid dispersions, solid lipid nanocapsules and NCs with the aim of improving the biopharmaceutical and pharmacokinetic behaviour of ABZ, ultimately increasing the plasma exposure to the active metabolite RBZ (Castro et al., 2010; Castro et al., 2013; Pensel et al., 2015; Paredes et al., 2016; Paredes et al., 2018a; Paredes et al., 2018b). Moreover, these formulations were tested in animal models of cystic echinococcosis showing partially improved efficacy (Pensel et al., 2014; Pensel et al., 2015; Pensel et al., 2018). Therefore, we believe that there is still substantial potential for the development of new alternatives to expand the therapeutic armamentaria against parasitic diseases.

In this work, we produced for the first time RBZ-NCs for oral administration using media milling and spray drying. The variables affecting the formulation process were explored and physicochemical analyses were performed in order to characterize the systems. Furthermore, we carried out a pharmacokinetic comparison between the novel formulation, a micronized form of the drug (mRBZ) and a PM using dogs as an experimental model.

2. Materials and methodology

2.1. Materials

mRBZ of 99.5% purity and a particle size of 1.08 ± 0.45 μm was purchased from Todo Droga® (Córdoba, Argentina), Poloxamer 188 (P188) was obtained from Rumapel, a sales representative from BASF (Buenos Aires, Argentina) and ultrapure water was used for all the assays and measurements (HF-Super Easy Series, Heal Force, Shanghai, China). For the milling process, Zirmil® Yttria-stabilized zirconia beads of 0.15–0.28 mm (Saint-Gobain ZirPro Kölh, Germany), were used. Transparent hard gelatine capsules (size 0) for the dissolution study were purchased from Todo Droga (Córdoba, Argentina), and the

dissolution medium was prepared with HCl 37% v/v (Sigma Aldrich). HPLC grade reagents were used for all chromatographic determinations. All other chemicals used in this work were of analytical grade.

2.2. Preparation of RBZ NSs (RBZ-NSs)

RBZ-NSs were prepared by media milling using a NanoDisp® laboratory-scale mill (NanoDisp®, Córdoba, Argentina). The device consisted of a sealed jacketed grinding chamber and a shaft coupled to a motor with variable speed. The temperature of the process was fixed at 20 °C by circulation of cold water with a Thermo Haake® compact refrigerated circulator (Thermo Fisher Scientific, USA). In the first place, mixtures of mRBZ and P188 in ratio 1:1 were ground in a mortar and ultrapure water was added gradually up to 200 mL to form suspensions with drug concentrations of 2.5, 5, 7.5 and 10% w/v (total solid contents: 5, 10, 15 and 20% w/v respectively). The resultant mixture was transferred to beaker, and magnetic stirred for 10 min. Afterwards, drug suspensions and zirconia beads (10, 17.5 and 25% v/v) were placed in the milling chamber and processed at 800 and 1600 rpm for 2 h. Samples were taken every 30 min for particle size and polydispersity index (PDI) evaluation.

2.3. Solid RBZ-NCs production

The water of RBZ-NSs was removed by spray drying using the experimental set-up reported in a previous work (Paredes et al., 2016). Briefly, samples were processed in a mini spray-drier Büchi B-290 (Büchi Labortechnik AG, Flawil, Switzerland) equipped with a dehumidifier module, and the processing conditions were: inlet temperature, 45 °C; atomizing air flow, 819 L/h; pump speed, 2 mL/min, aspiration, 75%. The obtained powders were weighed for process yield and moisture determination, and stored in dry conditions for further characterization.

2.4. Physical mixture

For the physicochemical characterization, dissolution and pharmacokinetic studies, a PM was used as a control. This was prepared in an agate mortar by gently mixing mRBZ and P188 in a 1:1 mass ratio for 3 min. After the preparation of the PM, the drug particle size was 1.10 ± 0.11 μm.

2.5. Process yield

To calculate the process yield (PY) after water removal, the dry basis of the NSs (drug and P188) was considered as theoretical 100%, and the following equation was used:

$$PY: Recovered\ solids\,(g)/Theoretical\ initial\ solids\,(g)x100\% \qquad (1)$$

2.6. Moisture content

Sample humidity was determined immediately after water removal. To this purpose, 0.5 g of the powders were placed in aluminium sample holders and processed at 90 °C in a halogen heating autoanalyzer (Ohaus M45®, Greifensee, Switzerland).

2.7. Particle size and zeta potential

Particle size distributions, polydispersity indexes and zeta potentials were determined in a Zetasizer® Nano ZS 90 (Malvern Instruments, UK). For measurements, 10 μL of NS or ~ 5 mg of NCs powder were mixed with 5 mL of water, manually dispersed to obtain suitable laser intensity, and placed into a quartz cell. For PM evaluation, 10 mg of powder were dispersed in 5 mL of water using a sonication bath for 10 min. Determinations were made at 25 °C (equilibration time: 3 min).

Values were expressed as mean values ± standard deviation (mean ± SD, n = 3).

2.8. Scanning electron microscopy

Photomicrographs of mRBZ, the PM and RBZ-NCs were taken by scanning electron microscopy (SEM) using a ZEISS instrument (Oberkochen, Germany). Powdered samples were placed upon aluminium studs and sputtered with Au before examination. Magnification ranges between 500 and 14,000X were used to observe the morphology of the particles.

2.9. Differential scanning calorimetry and thermogravimetric analyses (DSC-TGA)

Samples (~5 mg) of mRBZ, PM and RBZ-NCs were placed in aluminium pans, and processed with a Discovery DSC 25P instrument (TA Instruments, New Castle, DE) under dynamic N_2 atmosphere (50 mL/min) at a heating rate of 10 °C/min in the temperature range of 25 to 250 °C. The DSC cell was calibrated with indium (mp 156.6 °C; ΔHfus = 28.54 J/g). The same samples were run in a TGA instrument (Discovery HP TGA, TA Instruments, New Castle, DE). TGA curves were obtained in the temperature range of 25–350 °C under dynamic N_2 atmosphere (50 mL/min) with a heating rate of 10 °C/min.

2.10. Powder X-ray diffraction (PXRD)

The crystallinity of the powdered mRBZ, the PM and RBZ-NCs was assessed in a a PANalytical X-Pert ProVR X-ray powder diffractometer (PANalytical B.V., Almelo, Netherlands) with Cu Kα radiation, between 5° and 50° in 2θ in steps of 0.04 and counting time at 0.5 s per step.

2.11. Dissolution test

mRBZ, PM and RBZ-NCs were loaded into transparent hard gelatine capsules and underwent a dissolution test using an apparatus 1 (SOTAX AT 7 Smart, Westborough, MA, USA). As dissolution medium, 900 mL of HCl 0.1 M were used, the temperature adjusted at 37 ± 0.5 °C, and the rotational basket speed, set at 75 rpm. For all the assays, for mRBZ, PM and RBZ-NCs, the amount of formulation assayed was equivalent to 50 mg of drug. Aliquots (5 mL) were taken at 5, 10, 15, 20, 30, 45, 60 and 120 min with reposition of fresh medium, 0.1 μm membrane filters (Sartorius Stedium Biotech GmbH, Germany) were used to retain the undissolved NCs inside the dissolution vessels. The amount of dissolved drug was quantified using a Thermo Evolution® 300 UV–Vis spectrophotometer (Waltham, MA, USA) at a wavelength of 260 nm. All dissolution assays were performed in triplicate.

2.12. Pharmacokinetic trial

Nine free parasite and healthy (2–5-year-old) crossbreed dogs (6 non-pregnant females and 3 males) weighing 17.5 ± 4.5 kg were used in this trial. Animals were group housed in the same conditions and fed 12 h before and after the treatment with a Royal Canin® diet. Experimental dogs were randomly allocated into 3 groups (n = 3) (Group I: animals #1, #2, #3; Group II: animals #4, #5, #6, Group III: animals #7, #8, #9), which received three different treatments using a 3x3 crossover design. Each experimental treatment was given orally in hard gelatine capsules to the nine animals at a fixed dose of 10 mg/kg in three phases as shown in Table 1.

After administration, 2 mL blood samples were collected from the jugular vein using a 21 G, 1″ needle before administration (time 0) and at 0.25, 0.5 0.75, 1, 1.5, 2, 3, 4, 6, 8, 12, 16, and 24 h post-administration of the respective formulations. Blood samples were immediately transferred into heparinized tubes and centrifuged at 2000 × g for 15 min; the recovered plasma was stored at −20 °C until analysis by HPLC.

2.12.1. Purification of RBZ and analytical quantification methodology

RBZ was extracted from plasma using disposable C18 columns. To this purpose, 10 μL of OBZ (50 μg/mL) as internal standard were added to 500 μL of plasma in a glass test tube. Spiked samples were placed into a C18 column preconditioned with 0.5 mL of methanol followed by 0.5 mL water, in a vacuum system. Samples were washed (2 mL of water) and then eluted with 2 mL of HPLC-grade methanol. After elution, all samples were concentrated to dryness in a vacuum concentrator and then reconstituted with 200 μL of mobile phase.

RBZ quantification was performed in a Shimadzu 10 A system (Shimadzu Corporation, Kyoto, Japan) equipped with UV detection (Shimadzu, SPD-10A UV detector), using a Kromasil C18 column (5 μm, 250 mm 4.60 mm, Eka Chemicals, USA). The HPLC conditions were: injection volume, 50 μL; flow rate, 1.2 mL/min; column temperature, 25 °C; maximum absorbance, 291 nm. The mobile phase was an acetonitrile (A)/ammonium acetate (25 mM, pH 6.6) (B) elution gradient (0 min ¼ A/B: 27/73; 7–15 min ¼ A/B: 45/55; 17–20 min ¼ A/B: 27/73). The compounds were identified by the retention times (minutes) of pure reference standards (RBZ: 4.15 min and Oxibendazole: 9.49). Plasma calibration curves for each analyte were constructed by least squares linear regression analysis giving a correlation coefficient (r^2) between 0.9987 and 0.9995. The lower limit of quantification (LoQ) of the method was 0.05 μg/mL and the upper quantification limit was 10 μg/mL.

The pharmacokinetic parameters of RBZ in plasma for each individual animal after the different treatments were fitted with PK Solution 2.0 software (Summit Research Services, OH, USA).

2.13. Statistical analyses

All data were processed in Microsoft® Excel® 2016 (Microsoft Corporation, Redmond, USA) and presented as means ± standard deviation (SD). GraphPad Prism® 6 (GraphPad Software, San Diego, California, USA) was used for the statistical analyses. The mean residence time was determined as AUMC/AUC. The mean plasma pharmacokinetic variables for RBZ obtained from the different groups were statistically compared using the non-parametric Kruskal-Wallis test. In all cases, p values < 0.05 were considered as significant.

2.14. Ethical considerations

Animal procedures and management protocols were approved by the Catholic University of Cordoba (UCC) Ethical Committee and were in compliance with the guidelines of the US National Research Council's for the Care and Use of Laboratory Animals (NRC-USA, 2011). Dogs were routinely monitored by clinically experienced staff from the UCC Veterinary Hospital where the study was carried out, to report any adverse reaction during the three phases of the trial.

3. Results and discussion

3.1. Production of RBZ nanosuspensions (RBZ-NSs)

RBZ-NSs were efficiently obtained by means the media milling technique and the effect of variables related to the fabrication process where evaluated. Despite the processing parameters and formulation composition assayed, a decreasing tendency in particle size and PDI was observed at increasing milling times (Fig. 1 A-C). The drug content influenced the milling efficiency, and the overall particle size and PDI values were found to increase at higher drug contents, i.e. at 2 h the particle sizes were 164.50 ± 0.90 nm, 192.35 ± 2.78 nm and 274.68 ± 3.13 nm for 2.5, 5 and 7.5% w/v of drug content. The sample corresponding to 10% w/v was found to be a thick material after the milling experiment and the particle size measurement were

Table 1

Experimental design for the 3-phases complete crossover pharmacokinetic study. Animals received all the treatments i.e. mRBZ, PM and RBZ-NCs. Between each phase, a withdrawal gap of 15 days was left.

	Animals								
	Group 1			Group 2			Group 3		
	#1	#2	#3	#4	#5	#6	#7	#8	#9
Phase I	mRBZ	mRBZ	mRBZ	PM	PM	PM	NCs	NCs	NCs
				15 days withdrawal period					
Phase II	NCs	NCs	NCs	mRBZ	mRBZ	mRBZ	PM	PM	PM
				15 days withdrawal period					
Phase III	PM	PM	PM	NCs	NCs	NCs	mRBZ	mRBZ	mRBZ

discarded for being outside the nanometer range and indicated as * in Fig. 1A. The formulation containing 2.5% w/v of drug was then processed at different rotation speeds (800 and 1600 rpm) and results are shown in Fig. 1B. A higher rotation speed produced markedly smaller particle sizes and PDIs, with the values corresponding to 2 h of milling being 245.20 ± 0.73 nm, 164.5 ± 0.90 nm, and PDIs of 0.143 ± 0.010, 0.134 ± 0.018 for 800 and 1600 rpm respectively. Afterwards, the suspension containing 2.5% w/v of drug was milled at 1600 rpm with increasing amounts of zirconia beads (10, 17.5 and 25% v/v). This parameter was found to strongly affect the nanonization process, given that significant differences in particle sizes and PDI were observed for the three assays. For example, after 2 h of milling with the lower bead content (10% v/v), the particle size was 555.25 ± 16.63 nm, and during particle size determinations, several particle populations were observed (data no shown), with this corresponding to a high PDI value (0.354 ± 0.037). Contrarily, the particle size of NSs prepared with 25% v/v of beads was 164.5 ± 0.90 nm, and a notable decrease in PDI (0.134 ± 0.003) was observed, with narrowly-monodispersed particle size distribution.

3.2. Preparation of redispersible RBZ-NCs powders via spray drying

After bead milling with 25% v/v of beads at 1600 rpm, NSs containing increasing drug and P188 proportions, were processed by spray drying, and the redispersion capacity of the RBZ-NCs powders assayed in terms of particle size, PDI and zeta potential. These results, together with the spray drying process yield and moisture content of the final powders are presented in Table 2. Greater differences between the particle sizes and PDI values were observed before and after spray drying when the amount of total solids was increased in the NS. For instance, the lowest solid content permitted the redispersion of RBZ nanoparticles with a size of 181.30 ± 5.93 nm, meaning that the difference was only of ~ 17 nm when compared to the pre-dried NS. PDIs showed a similar trend, being 0.134 ± 0.018 for the NS and 0.152 ± 0.015 for the redispersed NCs. The rapid autodispersion of the RBZ-NCs powdered form obtained from the NS with 5% solid content is illustrated in Fig. 2. Conversely, powders containing greater amounts of RBZ and P188 presented decreased redispersion capacity, and NCs particle sizes and PDIs were two and even three-fold higher than those observed for the correspondent NSs. Moreover, the zeta potentials of the fresh NSs were negative in all cases, with values ranging between −10.1 and −13.7 mV, whereas the redispersion of NCs resulted in similar surface charge properties.

The spray drying PY was also affected by the amount of solids in the NSs, showing a decreasing trend for higher solid percentages. The best PY was achieved with the 5% NS, while a sharp product loss was observed for the 10, 15 and 20% NSs. The MC of spray dried powders was bellow 4% in all cases. The formulation corresponding to 5% of solids (2.5% of drug) was chosen to continue with further studies as it showed the smallest particle size and PDI, the best redispersion capacity, and the highest PY.

3.3. DSC-TGA analyses

Relevant information on the crystalline properties of mRBZ, P188, PM and RBZ-NCs was obtained by DSC. As shown in Fig. 3A, P188 and the pure drug presented well-defined endothermic melting peaks at 52 °C and 238 °C respectively, indicating a high degree of crystallinity in both samples. Although the event corresponding to the melting of P188 was also observed as sharp and less intense peak in the PM and RBZ-NCs, the peak corresponding to the drug was found to be poorly defined slightly shifted respect to that from the PM. Comparing the DSC thermograms of the PM and NCs, neither significant differences nor new peaks indicating glass transition or recrystallization were observed.

As shown in Fig. 3B, the thermogravimetry remained unchanged for all samples between 25 and 200 °C and the weight loss up to this point was in fact unnoticeable, corresponding to a low moisture content in the samples, which is in agreement with the results presented in Table 2. Even though P188 showed to be stable up to high temperatures, RBZ decomposition started at 200 °C, indicating that the melting of the compound takes place simultaneously with its decomposition. The PM and NCs thermograms evidenced a decomposition rate of RBZ relatively slower than those observed for P188 and the drug.

3.4. Fourier transformed infrared spectrometry (FTIR)

FTIR spectrometry analyses was used to evaluate the chemical structure of the drug and P188 in their pure forms as well as in the PM and RBZ-NCs. As shown in Fig. 4, all the characteristic peaks of RBZ were present in all the samples, i.e. at 1750 cm^{-1}, the peak corresponding to the stretching of the carboxyl group (C═O) and at 1600 cm^{-1}, stretching of N–H bond were observed unchanged for the pure drug, the PM and NCs. These findings indicate that no chemical interactions occurred between the drug and the stabilizer during the fabrication process.

3.5. Powder X-ray diffraction assay

Powder X-ray diffraction patterns of mRBZ, P188, PM and RBZ-NCs are shown in Fig. 5. mRBZ displayed a crystalline pattern with some of the characteristic peaks being at 10.5, 18.5, 23.3, 25.2, 26.5 and 27.7 °2θ (marked with arrows in Fig. 5), while P188 presented less crystalline characteristics, with only two main peaks at 19.5 and 23.3 °2θ. Importantly, in both the PM and RBZ-NCs, the respective characteristic peaks of mRBZ were found, indicating that neither amorphization nor formation of polymorphs resulted from the fabrication process.

3.6. Scanning electron microscopy

SEM analyses revealed that mRBZ particles are aggregated in clusters with heterogeneous particle sizes within the range of 5 and 20 μm (Fig. 6 A), nonetheless, a closer look permitted to evidence that those aggregates were formed with drug particles with a size of ~2 μm (Fig. 6
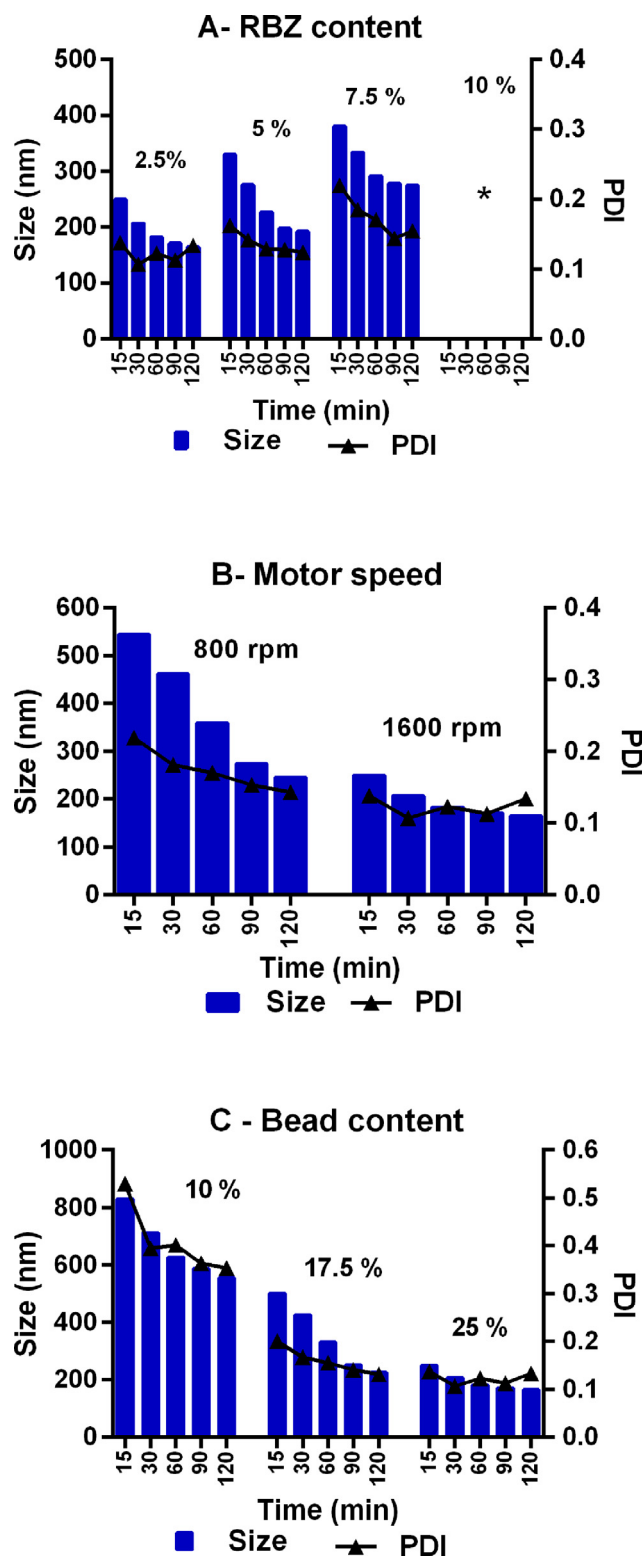
A- RBZ content

B- Motor speed

C - Bead content

Fig. 1. A – Milling experiment at increasing drug proportions, *particles were out of the nanometer range. B – Effect of the motor speed (800 and 1600 rpm) in the milling process. C – Evaluation of the milling process at different amount of zirconia beads (2.5, 5, 7.5 and 10% v/v).

B). The RBZ-NCs sample presented the typical sphere-like particles with smooth surface observed in spray dried powders as shown in Fig. 6 C, additionally, solid links can be distinguished among the spherical particles. At a greater magnification (Fig. 6 D), the surface of these particles is found to be rougher, and the presence of small grains

demonstrates that the RBZ-NCs are homogeneously distributed in the microcomposites. Additionally, P188 presented round particles of approximately 400 μm with a smooth surface (Fig. 6 E), whereas the PM was formed by heterogeneous agregates between broken granules of P188 and mRBZ (Fig. 6E). These results are in agreement with those observed in the redispersion assays in Section 3.2.

3.7. Dissolution assay

The dissolution rates of mRBZ, PM and RBZ-NCs were assayed in HCl 0.1 N at 37 °C. As observed in Fig. 7, no relevant differences between the PM and NCs were observed since both samples achieved a maximum dissolved amount of drug of 76.45 ± 3.21 and 77.87 ± 3.43% respectively at 120 min. The pure drug presented a slow dissolution rate, achieving only a maximum of 35.66 ± 1.05% of RBZ dissolved in the evaluated period.

3.8. Pharmacokinetic evaluation

RBZ (ABZO) concentrations in plasma were determined after a single oral administration of RBZ 10 mg/kg in the form of mRBZ, PM and RBZ-NCs. The comparative pharmacokinetic profiles and the correspondent parameters are displayed in Fig. 8 and Table 3 respectively. The cohorts treated with PM and the pure drug presented similar mean plasma concentration profiles with comparable values of area under the curve ($AUC_{0-\infty}$). Similarly, the maximum mean plasma concentrations (C_{max}) and T_{max} were no statistically different for mRBZ and PM (Kruskal-Wallis test $p > 0.05$). In comparison to the control groups, those dogs treated with RBZ-NCs displayed a significantly increased plasma exposure (Kruskal-Wallis test $p < 0.01$), with an $AUC_{0-\infty}$ value 1.76- and 1.9-fold higher than mRBZ and the PM respectively. Importantly, the C_{max} value was 1.59- and 1.5-fold superior to those observed for the control cohorts mRBZ and PM respectively (Kruskal-Wallis test $p < 0.05$). RBZ was detected in concentrations above the LoQ of the HPLC system after 20 h post-administration, whereas at 24 h, the experimental endpoint of this study, the concentrations of the drug were below the LoQ.

4. Discussion

The improvement of the biopharmaceutical and pharmacokinetic performance of poorly soluble drugs may lead to an improved efficacy, thus requiring less dose levels and potentially decreasing the risk of drug side effects. In this work, we aimed at the development of an optimized RBZ formulation for oral administration using the approach of nanonization.

In the first part of the work, mRBZ was transformed in to NCs by media milling, a highly flexible technique widely used in pharmaceutical industries (Mohammad et al., 2019). Different aspects related to the formulation might affect the efficacy of the milling process on achieving the desired particle size. In this sense, the drug and stabilizer content in the initial slurry play a key role on particle size reduction, given that increased solid contents produce higher viscosities, reduced mobility of the beads in the milling chamber and consequently a slower particle breakage (Afolabi et al., 2014). Our results are in line with this, as lower solid percentages in the initial suspension allowed to obtain finer particle sizes, whereas the formulation corresponding to 10% of drug and 10% P188 presented a semisolid consistency after the milling process with a particle size outside the nanometer range. It is worthy to remark that based on previous research (Paredes et al., 2016), we have kept a ratio 1:1 between drug and stabilizer P188 in order to achieve the smallest particle size possible while ensuring a complete redispersion of powders obtained after spray drying of the resultant NSs. During media milling, a number of factors related to the process lead to a reduction in the drug particle size, namely shearing, pressure, zirconia beads collisions and mechanical attrition (Chen et al., 2011; Juhnke

Table 2

Particle size, polydispersity index (PDI) and zeta potential values of RBZ-NCs formulations with increasing solid contents (drug and stabilizer) before and after spray-drying (redispersion). Values are expressed as mean ± SD (n = 3). Process yield (PY) and moisture content (MC) of final powders are also informed. ** The formulation containing 20% of solids was not suitable for DLS determinations.

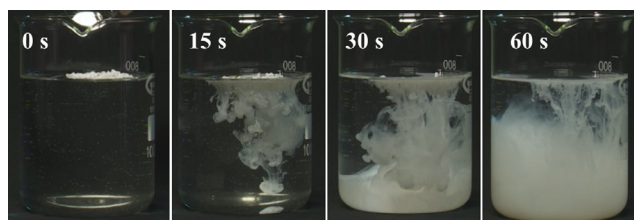| Solid content (% w/v)	Before spray drying			After spray drying				
	Size (nm)	PDI	Zeta Potential (mV)	Size (nm)	PDI	Zeta Potential (mV)	PY (%)	MC (%)
5	164.50 ± 0.90	0.134 ± 0.018	−10.3 ± 0.2	181.30 ± 5.93	0.152 ± 0.015	−9.6 ± 0.1	74.35 ± 6.46	1.69 ± 0.53
10	192.35 ± 2.78	0.124 ± 0.008	−11.7 ± 0.3	376.70 ± 32.00	0.275 ± 0.027	−10.5 ± 0.5	55.21 ± 3.11	2.3 ± 0.47
15	274.68 ± 3.13	0.155 ± 0.014	−12.8 ± 0.9	759.32 ± 26.70	0.312 ± 0.043	−11.5 ± 1.3	23.56 ± 2.06	2.8 ± 0.22
20	**	**	**	**	**	**	15.87 ± 4.18	3.5 ± 0.36

Fig. 2. Illustrative images of the water spontaneous redispersion of the powdered RBZ-NCs form obtained from the NS with 5% solid content. Pictures were taken at 0, 15, 30 and 60 s.

et al., 2012). In our experiments, increased bead concentrations and rotation frequencies (motor speed) were associated with lower particle sizes and PDI, with these results being related to an increase in the specific energy in the system and the milling intensity as explained in the literature (Afolabi et al., 2014).

Among the strategies used to remove water from nanoparticle suspensions, spray drying is widely accepted due to its rapidity, cost-effectiveness and ease for scale-up (Sosnik and Seremeta, 2015). After the transformation of RBZ-NSs into spray dried powders, the influence of solid content on the redispersion capacity was evaluated. Even though the capacity of P188 to exert a "cryoprotectant effect" in spray dried nanocrystals was explained in previous reports for low solids concentrations (Paredes et al., 2016), here we found out that this ability is limited at greater solid contents. This might be explained by the irreversible aggregation that occurs in the pneumatic atomizer of the drier, where the shearing forces produced increase the kinetic energy of nanoparticles, and therefore the number of collisions among particles, damaging the surfactant layer that surrounds them. Reasonably, an increasing number of particles in the atomized droplets, augment the chances of this phenomenon to take place.

The progressive decrease in the process yield when the percentage of solids became greater is explained by the adhesion of the material to the walls of the spray drier, and in particular to the cyclone, where particles still wet crashed and get stuck. This lack of drying efficiency is
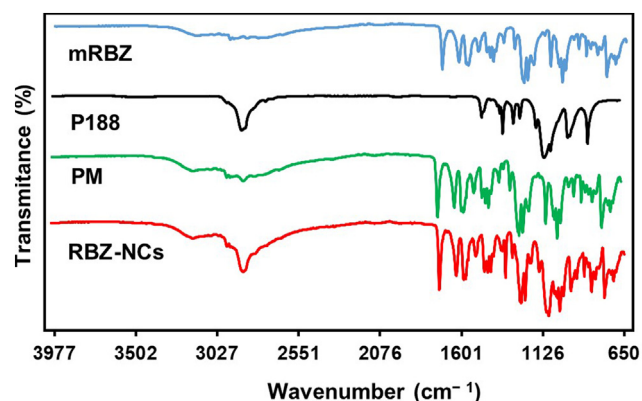

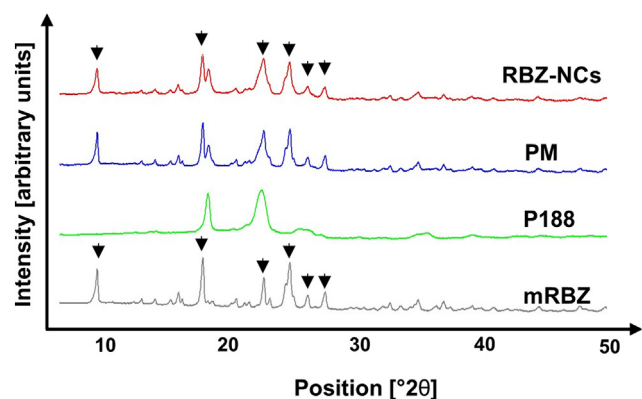**Fig. 4.** Fourier transformed infrared (FTIR) spectrometry of mRBZ, P188, PM and RBZ-NCs.

Fig. 5. Powder X-ray diffraction patterns obtained for RBZ-NCs, PM, P188 and mRBZ.
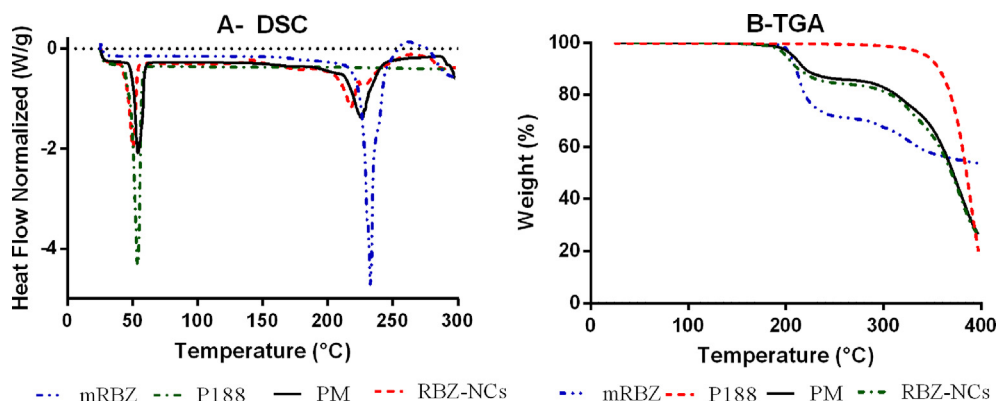

Fig. 3. A – Differential Scanning Calorimetry (DSC) of mRBZ, P188, PM and RBZ-NCs. B – Thermogravimetric analyses (TGA) of mRBZ, P188, PM and RBZ-NCs.
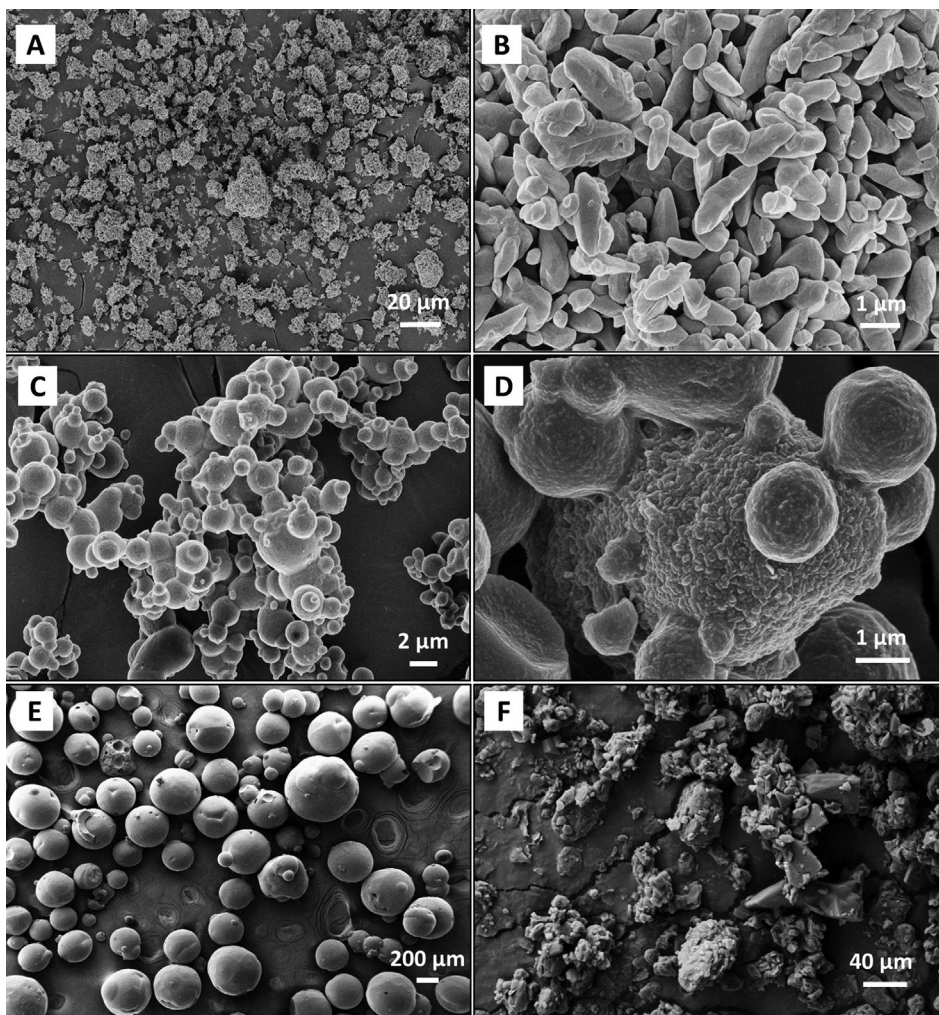
Fig. 6. Scanning electron microscopy images at different magnifications of A – mRBZ particles at 557X, B – mRBZ particles at 10.50 KX, C – RBZ-NCs at 2.8 KX, D – RBZ-NCs at 13.59 KX, E – P188 at 24X and F – PM at 200 X.
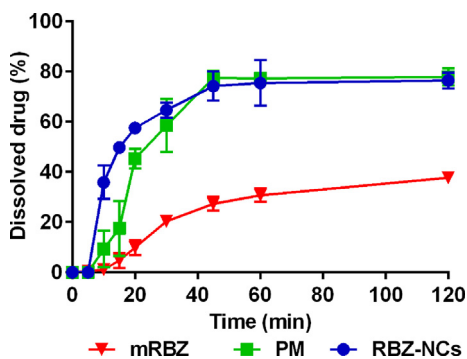

Fig. 7. Dissolution profile of mRBZ, PM and RBZ-NCs in HCl 0.1 M using apparatus 1 at 100 rpm at 37 °C at a dose of 50 mg of RBZ.
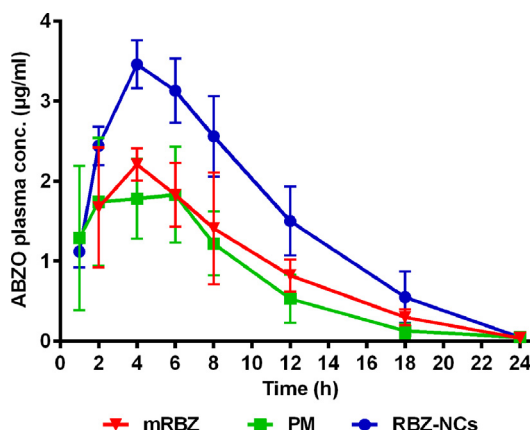

Fig. 8. Pharmacokinetic profile of mRBZ, PM and RBZ-NCs in dogs after administration of a single dose of 10 mg/kg in a complete crossover design. Values are informed in terms of mean ± standard deviation (n = 9).

undoubtedly linked to the low inlet temperature, that was fixed at 45 °C to avoid P188 melting (at 52 °C), which in case to take place, might jeopardize the redispersion capacity of the final product an the process yield as we observed previously (data no shown). Despite the low temperature used, a high drying efficiency was observed for low solid content samples. It was achieved by increasing the contact surface of the atomized NS droplets by means the use of a high atomization air flow (819 L/h) and low feed rate (pump: 2 mL/min). Likewise, a 75% of aspiration produces a slow circulation of the recently formed particles in the system, prolonging their contact with the air stream (Aloisio

et al., 2019).

The physicochemical characterization of RBZ-NCs showed that the manufacture process did not affect the drug properties. Although DSC analyses showed a decrease in the intensity of the melting peaks of RBZ in both PM and NCs, this was attributed to a partial amorphization of the drug during the analyses. Here, the heating ramp produced the

Table 3

Pharmacokinetic parameters obtained for mRBZ, PM and RBZ-NCs in dogs after administration of a single dose of 10 mg/kg in a 3x3 crossover design. Values are informed in terms of mean ± standard deviation (n = 9). T½ ab: absorption half-life; C_{max}: peak plasma concentration; T_{max}: time at C_{max}; $AUC_{0-\infty}$: area under the concentration vs time curve extrapolated to infinite; AUMC: area under the first moment concentration vs time curve extrapolated to infinite; T½el: elimination half-life; MRT: mean residence time. [a] Significantly different from both control cohorts mRBZ and PM, p < 0.05 Kruskal-Wallis test. [b] Significantly different from both control cohorts mRBZ and PM, p < 0.01 Kruskal-Wallis test.

PK Parameter	mRBZ	PM	RBZ-NCs
T ½ ab (h)	1.48 ± 0.65	0.95 ± 0.88	1.56 ± 0.21
C_{max} (µg/mL)	2.25 ± 1.63	2.39 ± 1.86	3.59 ± 0.68[a]
T_{max} (h)	3.20 ± 1.85	2.83 ± 1.83	4.40 ± 0.80
$AUC_{0-\infty}$ (µg.h/mL)	21.1 ± 14.7	19.5 ± 11.1	37.4 ± 8.4[b]
AUMC (µg.h²/mL)	242 ± 142	155 ± 81.1	315 ± 54
T½el (h)	3.76 ± 1.00	5.41 ± 1.42	3.58 ± 0.76
MRT (h)	8.48 ± 1.08	8.70 ± 1.98	8.00 ± 0.92

early liquefaction of P188 (52 °C) and the partial dissolution of the drug, which ultimately led to a decreased crystallinity and a less intense melting peak (Simonazzi et al., 2018). In line with this, the maintenance of the crystalline features of mRBZ was further proofed by X-ray powder diffraction, where all the characteristic peaks of the drug were also observed in the final NCs formulation. Moreover, similar findings in the FTIR analysis demonstrated the absence of chemical interactions between the drug and the surfactant.

Benzimidazole drugs, including RBZ are weak bases in nature, and its solubility in the pH range 2–11 is negligible (Wu et al., 2005), therefore, their dissolution in the acidic environment of the stomach is a crucial step before their absorption in the first part of the duodenum (McKellar and Scott, 1990; Lanusse et al., 1993; Jones et al., 2006). Dissolution assays demonstrated an improvement in the *in vitro* biopharmaceutical performance of RBZ when formulated as NCs in comparison to mRBZ. This was reasonably in agreement with the data observed for other hydrophobic drugs when processed as NCs where the enlargement in the specific surface area, led to a faster dissolution of the drug, achieving a rapid saturation in the dissolutor vessels (Ige et al., 2013). Besides the exponential increase in the specific surface, the comminution of drugs to the nanometer range, leads to a magnification in the particle curvature and therefore, to a greater dissolution pressure, allowing to achieve higher saturation concentrations of the active as explained by Mauludin et al. (2009). Surprisingly, the dissolution profile of the PM was not significantly different in comparison to that observed for RBZ-NCs, which is hypothetically related to the fact that the drug is micronized as observed in Fig. 6B, and the surfactant effect of P188 in the microenvironment that surrounds the drug microparticles inside the gelatine capsules, improving their wettability upon contact with the dissolution media. This could also be previously observed in similar experiments with a PM of ABZ and P188 1:1 (Castro et al., 2013).

When NCs are administered orally, a large number of uncontrolled variables with influence on their *in vivo* behaviour come into play, for instance, a variable gastric pH, water, food and mucus content, and gastrointestinal motility are some of the most relevant (Liu et al., 2020). Particularly in dogs, the rapid gastrointestinal transit is detrimental for the absorption of benzimidazole compounds, given that the drug not dissolved in the stomach, will travel to the duodenum and be excreted unmodified in faeces (Jones et al., 2006). In this scenario, the rapid redispersion, homogenization with the gastric content (elimination of fasted/fed variation) and dissolution of RBZ-NCs (Lu et al., 2017), led to an improvement on their *in vivo* performance when compared to the micronized controls. Another factor improving the plasma exposure of the novel formulation was attributed to the possible presence of undissolved NCs in the duodenum, which differently from the micronized

powders are mucoadhesive (Mauludin et al., 2009; Fontana et al., 2018). Moreover, these NCs might be translocated through the duodenum membrane into the plasmatic circulation increasing the plasma exposure as explained in the literature (Guo et al., 2019; Liu et al., 2020). In line with this, similar discrepancies between the *in vitro* dissolution and the pharmacokinetic performance observed here for the PM, were also reported by other authors (Liu et al., 2013; Hou et al., 2017). Interestingly enough, our experiments demonstrated that a dose of 10 mg/kg of RBZ-NCs produced a plasma exposure 50% greater than that observed for a similar NCs-based formulation of ABZ at 25 mg/kg after oral administration in dogs (Paredes et al., 2018b).

To the best of our knowledge, this is the first report on the oral pharmacokinetic performance of RBZ NCs, and our studies revealed a superiority in plasma exposure for the novel formulation. This, together with the consequent distribution of RBZ to the entire body, could potentially lead to an increased therapeutic efficacy against a variety of parasites dwelling in different tissues.

5. Conclusions

A novel alternative for the treatment of a variety of helminth parasitic diseases, including soil-transmitted helminthiasis in small animals and potentially in humans arises from this work. Two versatile techniques widely accepted by the pharma-industry such as bead milling and spray-drying were used to obtain a redispersible nanocrystalline RBZ powder with a fine particle size distribution and a high process yield. No physical or chemical alterations were observed in the active after the NCs fabrication process, and the *in vivo* performance was improved for the novel formulation after a single dose oral administration to dogs. In our view, further experiments to assess the therapeutic response (clinical efficacy against different helminth parasites) for this novel NCs-based RBZ formulation are needed.

Declaration of Competing Interest

The authors declare that they have no known competing financial interests or personal relationships that could have appeared to influence the work reported in this paper.

Acknowledgments

References

Afolabi, A., Akinlabi, O., Bilgili, E., 2014. Impact of process parameters on the breakage kinetics of poorly water-soluble drugs during wet stirred media milling: a micro-hydrodynamic view. Eur. J. Pharm. Sci. 51, 75–86. https://doi.org/10.1016/j.ejps.2013.09.002.

Ahmadnia, S., Moazeni, M., Mohammadi-Samani, S., Oryan, A., 2013. In vivo evaluation of the efficacy of albendazole sulfoxide and albendazole sulfoxide loaded solid lipid nanoparticles against hydatid cyst. Exp. Parasitol. 135, 314–319. https://doi.org/10.1016/j.exppara.2013.07.017.

Aloisio, C., Bueno, M.S., Ponte, M.P., Paredes, A., Palma, S.D., Longhi, M., 2019. Development of solid self-emulsifying drug delivery systems (SEDDS) to improve the solubility of resveratrol. Ther. Deliv. 10, 626–641. https://doi.org/10.4155/tde-2019-0054.

Castro, S., Bruni, S., Lanusse, C., Allemandi, D., Palma, S., 2010. Improved albendazole dissolution rate in pluronic 188 solid dispersions. AAPS PharmSciTech 11, 1518–1525. https://doi.org/10.1208/s12249-010-9517-6.

Castro, S.G., Dib, A., Suarez, G., Allemandi, D., Lanusse, C., Sanchez Bruni, S., Palma, S.D., 2013. Comparative plasma exposure of albendazole after administration of rapidly disintegrating tablets in dogs. Biomed Res. Int. 2013. https://doi.org/10.1155/2013/920305.

Chen, H., Khemtong, C., Yang, X., Chang, X., Gao, J., 2011. Nanonization strategies for poorly water-soluble drugs. Drug Discov. Today 16, 354–360. https://doi.org/10.

1016/j.drudis.2010.02.009.

Chomel, B.B., 2008. Control and prevention of emerging parasitic zoonoses. Int. J. Parasitol. 38, 1211–1217. https://doi.org/10.1016/j.ijpara.2008.05.001.

Esch, K.J., Petersen, C.A., 2013. Transmission and epidemiology of zoonotic protozoal diseases of companion animals. Clin. Microbiol. Rev. 26, 58–85. https://doi.org/10.1128/CMR.00067-12.

Fontana, F., Figueiredo, P., Zhang, P., Hirvonen, J.T., Liu, D., Santos, H.A., 2018. Production of pure drug nanocrystals and nano co-crystals by confinement methods. Adv. Drug Deliv. Rev. 131, 3–21. https://doi.org/10.1016/j.addr.2018.05.002.

Gao, L., Liu, G., Ma, J., Wang, X., Zhou, L., Li, X., 2012. Drug nanocrystals: in vivo performances. J. Control. Release 160, 418–430. https://doi.org/10.1016/j.jconrel.2012.03.013.

Guo, Mengran, Wei, M., Li, W., Guo, Meichen, Guo, C., Ma, M., Wang, Y., Yang, Z., Li, M., Fu, Q., Yang, L., He, Z., 2019. Impacts of particle shapes on the oral delivery of drug nanocrystals: Mucus permeation, transepithelial transport and bioavailability. J. Control. Release. https://doi.org/10.1016/j.jconrel.2019.06.015.

Hou, Y., Shao, J., Fu, Q., Li, J., Sun, J., He, Z., 2017. Spray-dried nanocrystals for a highly hydrophobic drug: increased drug loading, enhanced redispersity, and improved oral bioavailability. Int. J. Pharm. 516, 372–379. https://doi.org/10.1016/j.ijpharm.2016.11.043.

Ige, P.P., Baria, R.K., Gattani, S.G., 2013. Fabrication of fenofibrate nanocrystals by probe sonication method for enhancement of dissolution rate and oral bioavailability. Colloids Surfaces B Biointerfaces 108, 366–373. https://doi.org/10.1016/j.colsurfb.2013.02.043.

Jones, D.G., Bruni, S., Pharmacological, Q.A., 2006. Pharmacological approaches towards rationalizing the use of endoparasitic drugs in small animals. Vet. Pharmacol. Ther. 29, 443–457. https://doi.org///doi.org/10.1111/j.1365-2885.2006.00806.x.

Juhnke, M., Märtin, D., John, E., 2012. Generation of wear during the production of drug nanosuspensions by wet media milling. Eur. J. Pharm. Biopharm. https://doi.org/10.1016/j.ejpb.2012.01.005.

Lacey, E., 1990. Mode of action of benzimidazoles. Parasitol. Today 6, 112–115. https://doi.org/10.1016/0169-4758(90)90227-U.

Lanusse, C.E., Campus, M., De Bellevue, S., 1993. Gastrointestinal distribution of albendazole metabolites following netobimin administration to cattle: relationship with plasma disposition kinetics. J. Vet. Pharmacol. Ther. 16, 38–47. https://doi.org/10.1111/j.1365-2885.1993.tb00287.x.

Lanusse, C.E., Prichard, R.K., 1993. Clinical pharmacokinetics and metabolism of benzimidazole anthelmintics in ruminants. Drug Metab. Rev. 25, 235–279. https://doi.org/10.3109/03602539308993977.

Liu, G., Zhang, D., Jiao, Y., Guo, H., Zheng, D., Jia, L., Duan, C., Liu, Y., Tian, X., Shen, J., Li, C., Zhang, Q., Lou, H., 2013. In vitro and in vivo evaluation of riccardin D nanosuspensions with different particle size. Colloids Surfaces B Biointerfaces. https://doi.org/10.1016/j.colsurfb.2012.09.006.

Liu, J., Tu, L., Cheng, M., Feng, J., Jin, Y., 2020. Mechanisms for oral absorption enhancement of drugs by nanocrystals. J. Drug Deliv. Sci. Technol. 56, 101607. https://doi.org/10.1016/j.jddst.2020.101607.

Lu, Y., Qi, J., Dong, X., Zhao, W., Wu, W., 2017. The in vivo fate of nanocrystals. Drug Discov. Today 22, 744–750. https://doi.org/10.1016/j.drudis.2017.01.003.

Mauludin, R., Müller, R.H., Keck, C.M., 2009. Development of an oral rutin nanocrystal formulation. Int. J. Pharm. 370, 202–209. https://doi.org/http://dx.doi.org/10.1016/j.ijpharm.2008.11.029.

McKellar, Q., Scott, E.W., 1990. The benzimidazole anthelmintic agents: a review. J. Vet. Pharmacol. Ther. 13, 223–247. https://doi.org/10.1111/j.1365-2885.1990.tb00773.x.

Mohammad, I.S., Hu, H., Yin, L., He, W., 2019. Drug nanocrystals: Fabrication methods and promising therapeutic applications. Int. J. Pharm. 562, 187–202. https://doi.org/10.1016/j.ijpharm.2019.02.045.

Möschwitzer, J.P., 2013. Drug nanocrystals in the commercial pharmaceutical development process. Int. J. Pharm. 453, 142–156. https://doi.org/10.1016/j.ijpharm.2012.09.034.

Naseri, M., Akbarzadeh, A., Spotin, A., 2016. Scolicidal and apoptotic activities of albendazole sulfoxide and albendazole sulfoxide-loaded PLGA-PEG as a novel nanopolymeric particle against Echinococcus granulosus protoscoleces. Parasitol. Res. https://doi.org/10.1007/s00436-016-5250-8.

NRC-USA, 2011. Guide for the Care and Use of Laboratory Animals, Guide for the Care and Use of Laboratory Animals. https://doi.org/10.17226/12910.

Page, S.W., 2008. Antiparasitic Drugs, in: Stephen W Page and Jill E Maddison (Ed.), Small Animal Clinical Pharmacology. Elsevier B.V., Philadelphia, pp. 198–260.

Paredes, A.J., Bruni, S.S., Allemandi, D., Lanusse, C., Palma, S.D., 2018a. Albendazole nanocrystals with improved pharmacokinetic performance in mice. Ther. Deliv. 9. https://doi.org/10.4155/tde-2017-0090.

Paredes, A.J., Litterio, N., Dib, A., Allemandi, D.A., Lanusse, C., Bruni, S.S., Palma, S.D., 2018b. A nanocrystal-based formulation improves the pharmacokinetic performance and therapeutic response of albendazole in dogs. J. Pharm. Pharmacol. 70. https://doi.org/10.1111/jphp.12834.

Paredes, A.J., Llabot, J.M., Sánchez Bruni, S., Allemandi, D., Palma, S.D., 2016. Self-dispersible nanocrystals of albendazole produced by high pressure homogenization and spray-drying. Drug Dev. Ind. Pharm. 42. https://doi.org/10.3109/03639045.2016.1151036.

Pensel, P.E., Castro, S., Allemandi, D., Bruni, S.S., Palma, S.D., Elissondo, M.C., 2014. Enhanced chemoprophylactic and clinical efficacy of albendazole formulated as solid dispersions in experimental cystic echinococcosis. Vet. Parasitol. 203, 80–86. https://doi.org/10.1016/j.vetpar.2014.01.027.

Pensel, P., Paredes, A., Albani, C.M., Allemandi, D., Sanchez Bruni, S., Palma, S.D., Elissondo, M.C., 2018. Albendazole nanocrystals in experimental alveolar echinococcosis: Enhanced chemoprophylactic and clinical efficacy in infected mice. Vet. Parasitol. 251. https://doi.org/10.1016/j.vetpar.2017.12.022.

Pensel, P.E., Ullio Gamboa, G., Fabbri, J., Ceballos, L., Sanchez Bruni, S., Alvarez, L.I., Allemandi, D., Benoit, J.P., Palma, S.D., Elissondo, M.C., 2015. Cystic echinococcosis therapy: Albendazole-loaded lipid nanocapsules enhance the oral bioavailability and efficacy in experimentally infected mice. Acta Trop. https://doi.org/10.1016/j.actatropica.2015.09.016.

Permana, A.D., Tekko, I.A., McCrudden, M.T.C., Anjani, Q.K., Ramadon, D., McCarthy, H.O., Donnelly, R.F., 2019. Solid lipid nanoparticle-based dissolving microneedles: a promising intradermal lymph targeting drug delivery system with potential for enhanced treatment of lymphatic filariasis. J. Control. Release 316, 34–52. https://doi.org/10.1016/j.jconrel.2019.10.004.

Romero, G.B., Keck, C.M., Müller, R.H., 2016. Simple low-cost miniaturization approach for pharmaceutical nanocrystals production. Int. J. Pharm. 501, 236–244. https://doi.org/10.1016/j.ijpharm.2015.11.047.

Simonazzi, A., Cid, A.G., Paredes, A.J., Schofs, L., Gonzo, E.E., Palma, S.D., Bermúdez, J.M., 2018. Development and in vitro evaluation of solid dispersions as strategy to improve albendazole biopharmaceutical behavior. Ther. Deliv. 9, 623–638. https://doi.org/10.4155/tde-2018-0037.

Sosnik, A., Seremeta, K.P., 2015. Advantages and challenges of the spray-drying technology for the production of pure drug particles and drug-loaded polymeric carriers. Adv. Colloid Interface Sci. https://doi.org/10.1016/j.cis.2015.05.003.

Touzet, A., Pfefferlé, F., van der Wel, P., Lamprecht, A., Pellequer, Y., 2018. Active freeze drying for production of nanocrystal-based powder: a pilot study. Int. J. Pharm. 536, 222–230. https://doi.org/10.1016/j.ijpharm.2017.11.050.

WHO/OIE, 2002. Manual on Echinococcosis in Humans and Animals: A Public Health Problem of Global Concern, Veterinary Parasitology. https://doi.org/10.1016/S0304-4017(01)00631-8.

WHO, 2020. Soil-transmitted helminth infections [WWW Document]. URL https://www.who.int/news-room/fact-sheets/detail/soil-transmitted-helminth-infections (accessed 3.31.20).

Wu, Z., Tucker, I.G., Razzak, M., Medlicott, N.J., 2005. An in vitro kinetic method for detection of precipitation of poorly soluble drugs. Int. J. Pharm. 304, 1–3. https://doi.org/10.1016/j.ijpharm.2005.08.012.